

# SIMULATION OF THERMAL DECOMPOSITION OF MINERAL INSULATING OIL

V. G. M. Cruz<sup>1,2\*</sup>, A. L. H. Costa<sup>2</sup> and M. L. L. Paredes<sup>2</sup>

<sup>1</sup>Furnas Centrais Elétricas, Rua Real Grandeza 219, CEP: 22281-900, Rio de Janeiro - RJ, Brazil.  
Phone: + (55) (21) 2528-3073, Fax: + (55) (21) 2528-3111  
E-mail: vcruz@furnas.com.br

<sup>2</sup>Rio de Janeiro State University (UERJ), Instituto de Química, Rua São  
Francisco Xavier 524, CEP: 20550-900, Rio de Janeiro - RJ, Brazil.

(Submitted: May 28, 2014 ; Revised: October 16, 2014 ; Accepted: November 25, 2014)

**Abstract** - Dissolved gas analysis (DGA) has been applied for decades as the main predictive maintenance technique for diagnosing incipient faults in power transformers since the decomposition of the mineral insulating oil (MIO) produces gases that remain dissolved in the liquid phase. Nevertheless, the most known diagnostic methods are based on findings of simplified thermodynamic and compositional models for the thermal decomposition of MIO, in addition to empirical data. The simulation results obtained from these models do not satisfactorily reproduce the empirical data. This paper proposes a flexible thermodynamic model enhanced with a kinetic approach and selects, among four compositional models, the one offering the best performance for the simulation of thermal decomposition of MIO. The simulation results obtained from the proposed model showed better adequacy to reported data than the results obtained from the classical models. The proposed models may be applied in the development of a phenomenologically-based diagnostic method.

**Keywords:** Dissolved gas analysis; Mineral insulating oil; Thermal decomposition; Power transformer.

## INTRODUCTION

Mineral insulating oil (MIO) is a petroleum derivative widely employed in high voltage power transformers, especially in those of electric energy generation and transmission systems.

Due to the relevance of power transformers for electric systems and the high costs involved in their malfunctioning, predictive maintenance techniques have been developed and improved for the last 80 years (Rogers, 1978). These techniques aim to detect incipient faults in oil insulated transformers.

The most well known of these predictive maintenance techniques is Dissolved Gas Analysis (DGA). The DGA technique consists of sampling MIO from in-service equipment and quantifying the concentrations of some specific light compounds that are

produced through the cracking of the MIO molecules and remain dissolved in the liquid phase. The patterns formed by the set of these concentrations are then used to identify an existing incipient fault and to classify this fault through semi-empirical algorithms, known as diagnostic methods. This correlation between the dissolved gas concentration patterns and the incipient faults is possible since the rate of energy dissipated to the oil in the neighborhood of a faulty region implies a local temperature that determines which products will be predominant in the cracking reaction equilibrium (ASTM, 2007; ASTM, 2009; IEC, 2007; IEEE, 2009).

Nowadays, the diagnostic methods that are most applied by maintenance engineering personnel, referred to here as classical diagnostic methods, are described at the standards IEC 60599 (IEC, 2007)

---

\*To whom correspondence should be addressed

and IEEE C57.104 (IEEE, 2009), *i.e.*, the IEC, Duval, Rogers and Doernenburg methods. The algorithms for these methods are mainly based on the observations of Halstead's simplified thermodynamic study on MIO decomposition, published in 1973 (Halstead, 1973), and empirical data obtained from faulty transformers.

In his work, Halstead established a simple two-step model for the thermal decomposition of MIO: i) in a first step, the oil molecules are considered to react completely and degrade exclusively into six products, namely:  $H_2$ ,  $CH_4$ ,  $C_2H_6$ ,  $C_2H_4$  and  $C_2H_2$ , the so-called light compounds, and C(s) (graphite carbon); ii) in a second step, the equilibrium partial pressures in the system formed by these six species are calculated at different temperatures. The results are reported on a plot of partial pressure logarithms as functions of the equilibrium temperature. Although one can obtain valid trends from this logarithmic plot, the numerical values, when converted to a molar basis, deviate considerably from DGA data reported by IEC TC 10 (Duval and dePablo, 2001). The model predicts virtually only  $H_2$ ,  $CH_4$  and great amounts of C(s) in equilibrium for all temperatures, while IEC data may present significant quantities of all gases, depending on the incipient fault type. This deviation is probably related to the assumption of a thermodynamic equilibrium of totally decomposed oil molecules when, in fact, the equilibrium is not fully achieved (IEC, 2007; IEEE, 2009; Shirai *et al.*, 1977).

Besides Halstead's work, the technical literature presents another effort to develop a thermodynamic model for the thermal degradation of mineral insulating oil. In 1977, Shirai and co-workers proposed a model in which the insulating oil molecules are simply represented as the *n*-eicosane molecule. Equilibrium simulations were presented for a system containing  $C_{20}H_{42}$ ,  $H_2$ ,  $CH_4$ ,  $C_2H_6$ ,  $C_2H_4$ ,  $C_2H_2$ ,  $C_3H_8$  and  $C_3H_6$ . The authors observed that, when the C(s) species was included in the equilibrium system, the simulation results deviated significantly from empirical data. On the other hand, the suppression of the C(s) species led to more coherent results (Shirai *et al.*, 1977).

Although Shirai and co-workers' simulation results seem more adequate than those of Halstead when compared to IEC data, the formation of C(s) is an important empirical observation (IEC, 2007; IEEE, 2009) and should not be neglected. As mentioned before, the classical diagnostic methods are mainly based on Halstead's conclusions and few papers cite Shirai and co-workers' study.

Recently, most efforts in this area have been devoted to the development of the so-called intelligent or expert diagnostic systems and numerous papers have been published on this subject over the years (Lowe, 1985; Barrett, 1989; Tomsovic *et al.*, 1993; Zhang *et al.*, 1996; Wang and Liu, 1998; Huang, 2003; Fei *et al.*, 2009; Fei and Zhang, 2009; Wu *et al.*, 2011; Miranda *et al.*, 2012). The expert systems try to improve the classical methods' performances, commonly by combining the responses of two or more of these methods and/or applying artificial intelligence techniques to empirical databases. No actual research efforts on developing more suitable thermodynamic models for the thermal decomposition of MIO could be identified.

The present work proposes a more adequate thermodynamic modeling and evaluates four proposed compositional models for the thermal decomposition of MIO, since the models on which the classical diagnostic methods rely are not able to satisfactorily represent empirical data.

## TYPICAL INCIPIENT FAULT PATTERNS

Table 1 presents typical mole fraction ranges for each incipient fault type based on IEC data, the same database used in the preparation of IEC 60599:1999. IEC data consist of 117 sets of volumetric concentrations of gases dissolved in the MIO of faulty electrical equipment and their respective fault classification by visual inspections. Assuming ideal gas behavior for the mixture, in each reported case, the volumetric concentrations of the gases related to MIO decomposition, *i.e.*,  $H_2$ ,  $CH_4$ ,  $C_2H_6$ ,  $C_2H_4$  and  $C_2H_2$ , were normalized to obtain the mole fractions. Then, the lower confidence limit (LCL) and the upper confidence limit (UCL) for a 95% confidence level were calculated for all species of interest in each incipient fault type. In the current work, these typical incipient fault patterns will be used as references to assess the applicability of the proposed compositional models.

It is important to note that the information presented in the IEC data was not obtained from controlled experiments designed for this purpose. IEC data were constructed with information from in-service equipment and, therefore, they are subject to intrinsic errors related to the operational characteristics of the equipment and to the nature of the faults, such as non-ideal homogeneity of the MIO volume, accumulation of the dissolved gases over time and the possible existence of multiple simultaneous faults.

**Table 1: Typical mole fraction patterns for incipient faults.**

Gas	Partial discharges		Discharges of low energy		Discharges of high energy		Low/medium temperature thermal faults		High temperature thermal faults	
	LCL	UCL	LCL	UCL	LCL	UCL	LCL	UCL	LCL	UCL
H <sub>2</sub>	0.80	0.96	0.37	0.54	0.35	0.42	0.14	0.43	0.09	0.21
CH <sub>4</sub>	0.03	0.18	0.07	0.11	0.13	0.17	0.29	0.53	0.21	0.31
C <sub>2</sub> H <sub>6</sub>	0.00	0.02	0.01	0.04	0.02	0.03	0.05	0.24	0.05	0.16
C <sub>2</sub> H <sub>4</sub>	0.00	0.00	0.07	0.12	0.17	0.21	0.08	0.21	0.40	0.52
C <sub>2</sub> H <sub>2</sub>	0.00	0.00	0.24	0.42	0.22	0.28	0.00	0.01	0.01	0.04

## THERMODYNAMIC MODEL

Both thermal and electrical incipient faults occur in small areas and the dissipated energy concentrates in small volumes of the insulating oil, causing local temperatures to rise, thus originating hot spots in the oil. Equilibrium temperatures in these hot spots may be used as universal indicators to evaluate the criticality of the faults, no matter the type of these faults.

The thermodynamic modeling used here for chemical equilibrium calculations on the thermal decomposition of MIO is based on the method of Lagrange multipliers for minimization of the system's Gibbs energy (Smith *et al.*, 2004). The study was carried out with two models: an unrestricted thermodynamic model and a carbon-optimized thermodynamic model.

The unrestricted thermodynamic model is composed of Eqs. (1) to (4), as follows:

$$\Delta G_{f,i}^{\circ}(T) + RT \ln \left( \frac{n_i}{n_t} \right) + \lambda_C a_{i,C} + \lambda_H a_{i,H} = 0 \quad (1)$$

$$\lambda_C = 0 \quad (2)$$

$$\sum_j n_j a_{j,C} - \sum_j n_j^0 a_{j,C} = 0 \quad (3)$$

$$\sum_j n_j a_{j,H} - \sum_j n_j^0 a_{j,H} = 0 \quad (4)$$

where the subscripts *C* and *H* stand, respectively, for carbon and hydrogen, subscript *j* indicates all species and subscript *i* indicates all species except C(s), superscript 0 stands for initial values and subscript *t* stands for total amount in the gas phase.  $\Delta G_{f,i}^{\circ}(T)$  is the standard Gibbs energy of formation as a function of temperature *T*, *R* is the gas constant, *n* is the amount of substance,  $\lambda$  is the Lagrange multiplier

and *a* is the atomic matrix containing the number of each element in the species.

In the carbon-optimized thermodynamic model, Eqs. (1), (3) and (4) are kept the same as in the unrestricted model. Also, to allow the restriction of the equilibrium amount of C(s), Eq. (2) is replaced by Eq. (5) and Eq. (6) is included, as follows:

$$\lambda_C + \lambda_R = 0 \quad (5)$$

$$n_C - n_{C,R} = 0 \quad (6)$$

where the subscript *R* stands for restriction (*i.e.*,  $n_{C,R}$  represents the quantity of solid carbon present at equilibrium).

The calculation of the standard Gibbs energy of formation of each species, for the specified temperatures, required previous knowledge of the standard enthalpy and Gibbs energy of formation at 298 K and the ideal gas constant-pressure heat capacity as a function of temperature for each species. Estimates of these thermodynamic properties for heavy species were obtained through Joback's group contribution method (Poling *et al.*, 2001). The same thermodynamic properties for the light species were obtained from the literature (Smith *et al.*, 2004).

The decomposition reactions were assumed to occur in the vapor phase. Therefore, when exposed to localized higher temperatures, the oil compounds evaporate and decompose into lighter species that dissolve in the liquid phase after equilibrium in the gas phase is achieved. No further reactions occur in the liquid phase. Ideal gas behavior was assumed for the gas phase and the total pressure of the system was assumed as 1 bar.

Equation (6) allows the carbon-optimized thermodynamic model to adapt to both Halstead's proposal, with unrestricted amount of C(s), and Shirai and co-workers' proposal, with the amount of C(s) restricted to zero. Also, the carbon-optimized model makes it

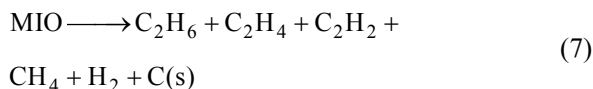
possible to simulate intermediate scenarios by specification of intermediate amounts of C(s). Since MIO in the neighborhood of an incipient fault is not actually in thermodynamic equilibrium (IEC, 2007; IEEE, 2009; Shirai *et al.*, 1977), the kinetics of the phenomenon may be relevant and should not be neglected. The formation process of C(s) is assumed to be slower than the formation process of the gaseous species. Therefore, the limitation of the equilibrium amount of C(s) makes it possible to simulate MIO thermal decomposition in a stage that is closer to that occurring in a real system and, also, preserves the empirical observation (IEC, 2007; IEEE, 2009) of the formation of C(s). Therefore, the restriction on the equilibrium amount of C(s) is an equilibrium approach that takes into consideration, in some way, the kinetic contribution to the MIO thermal decomposition model.

## COMPOSITIONAL MODELS

Four systems were proposed to represent the local composition at the hot spots. Since C<sub>2</sub>H<sub>6</sub>, C<sub>2</sub>H<sub>4</sub>, C<sub>2</sub>H<sub>2</sub>, CH<sub>4</sub> and H<sub>2</sub> are commonly quantified and applied in the existing diagnostic methods, the presence of these species in the equilibrium systems is a minimum requirement for all proposals. Systems 1 and 2 were simply adapted from Halstead's and Shirai and co-workers' studies and contain 6 and 7 species, respectively. Systems 3 and 4 are more complex systems and contain 60 and 81 species, respectively.

### System 1

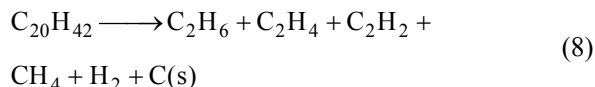
System 1 is based on Halstead's study. The MIO components are completely decomposed into lighter species and equilibrium occurs in this secondary system. Therefore, the equilibrium system is composed of the light compounds of most interest for diagnostic methods, *i.e.*, C<sub>2</sub>H<sub>6</sub>, C<sub>2</sub>H<sub>4</sub>, C<sub>2</sub>H<sub>2</sub>, CH<sub>4</sub> and H<sub>2</sub> and a specified amount of C(s). The decomposition reaction can be described as follows:



### System 2

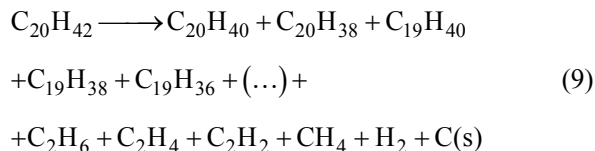
System 2 is based on Shirai and co-workers' study. MIO is represented by *n*-eicosane which is decomposed into lighter species. Differently from the cited study, in this work propane and propene are

suppressed, so *n*-eicosane decomposes exclusively into the light compounds of interest. The equilibrium system is composed of *n*-eicosane, the light compounds of interest and a specified amount of C(s). The decomposition reaction is listed below:



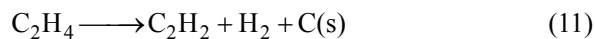
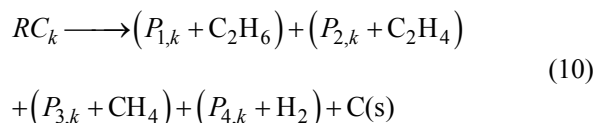
### System 3

System 3 is a more complete version of System 2. *n*-Eicosane still represents all compounds of MIO, but its decomposition leads to a complete series of straight alkanes, 1-alkenes and 1-alkynes, with the lengths of the carbon chains varying from 20 to 1. The equilibrium system consists of 60 species, as follows: 20 alkanes, 19 1-alkenes, 19 1-alkynes, H<sub>2</sub> and a specified amount of C(s). The decomposition reaction is represented below:



### System 4

System 4 is based on compositional information for MIO available in technical literature (ASTM, 1994). MIO is composed of thousands of substances and it is not practical to identify each one of them; therefore, the technical literature presents compositional information classifying the components in a few groups or families. System 4 relates each of 15 hydrocarbon families to 1 representative compound, as seen in Table 2. The decomposition of these representative compounds leads to the same 5 light compounds of interest plus 60 by-products and C(s) and it is assumed to occur in two stages: on stage one, the paraffinic chain of the representative compounds decomposes to C<sub>2</sub>H<sub>6</sub>, C<sub>2</sub>H<sub>4</sub>, CH<sub>4</sub>, H<sub>2</sub> and C(s) and, in stage two, C<sub>2</sub>H<sub>4</sub> decomposes to C<sub>2</sub>H<sub>2</sub>, H<sub>2</sub> and C(s). The equilibrium system consists of 81 species, as follows: 15 compounds representative of the families in the original MIO, 60 decomposition by-products, C<sub>2</sub>H<sub>6</sub>, C<sub>2</sub>H<sub>4</sub>, C<sub>2</sub>H<sub>2</sub>, CH<sub>4</sub>, H<sub>2</sub> and a specified amount of C(s). The decomposition scheme can be represented as follows, where *RC* is a representative compound, *P* is a decomposition product and subscript *k* is the associated representative compound index:



### NUMERICAL SIMULATION AND OPTIMIZATION

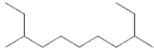
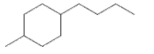
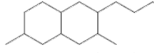
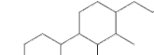
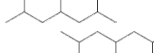

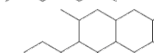

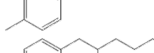
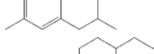
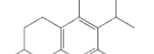

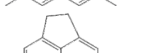
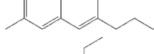
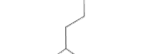
In order to compare the adequacy of the different proposed compositional models and also to evaluate

the performance of the proposed thermodynamic model in representing the thermal decomposition of MIO, numerical simulations and optimization problems were carried out according to the methodology described as follows.

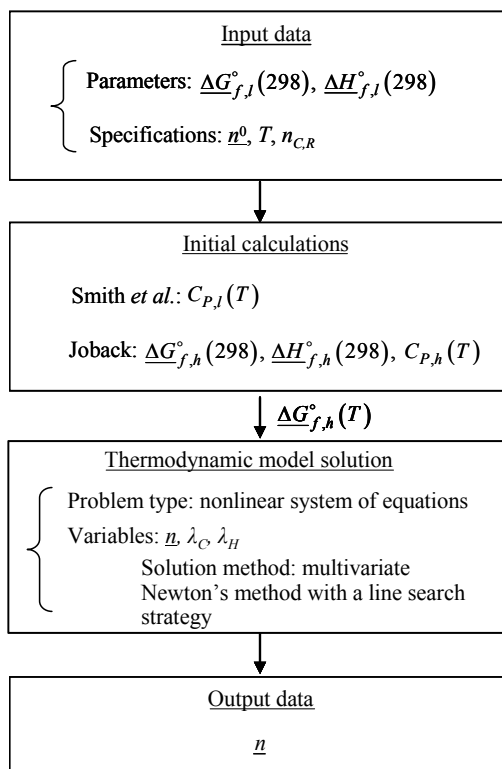
#### Numerical Simulation

Chemical equilibrium simulations were performed on the proposed systems with equilibrium temperatures ranging from 0 °C to 2000 °C, with 1 °C steps, and the restricted equilibrium amount of C(s) ranging from 0% to 100% of the unrestricted equilibrium amount of C(s), with 1% steps.

**Table 2: Representative compounds of hydrocarbon families in mineral insulating oil.**

Family	Composition (% by weight)	Representative Compound	Formula
isoparaffins	11.6		C <sub>13</sub> H <sub>28</sub>
1-ring naphthenes	16.5		C <sub>11</sub> H <sub>22</sub>
2-ring naphthenes	17.1		C <sub>16</sub> H <sub>30</sub>
3-ring naphthenes	12.4		C <sub>21</sub> H <sub>38</sub>
4-ring naphthenes	10.1		C <sub>26</sub> H <sub>46</sub>
5-ring naphthenes	4.0		C <sub>28</sub> H <sub>48</sub>
alkylbenzenes	5.0		C <sub>11</sub> H <sub>16</sub>
naphthene benzenes	6.1		C <sub>16</sub> H <sub>24</sub>
di-naphthene benzenes	7.5		C <sub>21</sub> H <sub>32</sub>
naphthalenes	4.2		C <sub>16</sub> H <sub>20</sub>
acenaphthenes	2.5		C <sub>17</sub> H <sub>20</sub>
fluorenes	2.1		C <sub>19</sub> H <sub>22</sub>
phenanthrenes	0.6		C <sub>21</sub> H <sub>24</sub>
pyrenes	0.1		C <sub>24</sub> H <sub>26</sub>
chrysenes	0.2		C <sub>26</sub> H <sub>28</sub>

The systems formed by the nonlinear equations of both the unrestricted and carbon-optimized thermodynamic models were solved for equilibrium compositions of each system through the multivariate Newton-Raphson method using a line search strategy through the golden section method (Press *et al.*, 2007). Figure 1 presents the algorithm of the carbon-optimized numerical simulation carried out for each pair of equilibrium temperature and restricted equilibrium amount of C(s), where  $\Delta H_f^\circ(298)$  is the standard enthalpy of formation at 298 K,  $C_p(T)$  is the ideal gas constant-pressure heat capacity as a function of temperature and subscripts  $l$  and  $h$  stand, respectively, for light and heavy species. The described simulation was carried out for all 202,101 possible pairs of temperature and amount of C(s), within their specified ranges and subdivisions.



**Figure 1:** Algorithm structure.

For purposes of comparison with the typical incipient faults patterns, the equilibrium amounts of substances obtained from each simulation were transformed into gas phase mole fractions of the dissolved gases of interest, namely:  $C_2H_6$ ,  $C_2H_4$ ,  $C_2H_2$ ,  $CH_4$  and  $H_2$ . All calculated mole fractions for a particular compositional model were saved in a 2001x101x5 hypermatrix for future consultations.

## Numerical Optimization

In order to enable qualitative and quantitative evaluations of the obtained simulation results, 117 two-dimensional optimization problems were solved to compare each one of the reported DGA patterns in IEC data to the mole fractions obtained from the simulations using a particular compositional model.

The optimization problems aimed to find the equilibrium temperatures and percentages of the equilibrium amounts of C(s) that minimized the summation of the squared relative residues between model predicted and reported mole fractions. As the mentioned objective function does not admit empirical mole fractions equal to zero, in such cases, the lower limit of detection of each gas was adopted, according to inter-laboratory studies conducted by ASTM (ASTM, 2003). A brute-force approach was applied in the solution of these problems, so all ranges of interest of temperature and percentage of equilibrium amount of C(s) could be examined, thus avoiding local minimum issues. The applied methodology consisted of calculating the summation of the squared relative residues between one IEC data DGA pattern and each calculated DGA pattern in the previously cited hypermatrix. The lowest among all 202,101 calculated values indicated the optimum pair of equilibrium temperature and percentage of the equilibrium amounts of C(s) to represent that IEC data DGA pattern.

Mean relative errors could be calculated from the objective function values.

## RESULTS AND DISCUSSION

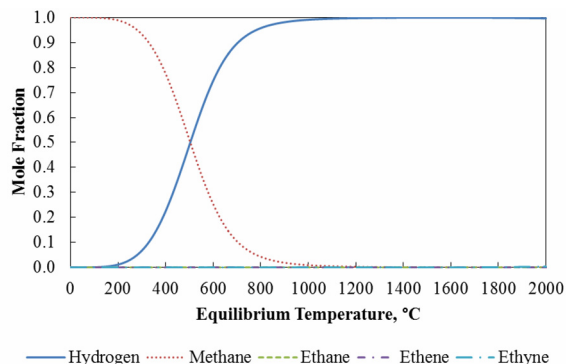
The results are presented in a logical manner and divided into main aspects of the problem, as follows: simulated mole fraction profiles, analysis of the proposed model performance, comparison of calculated and reported mole fractions and objective function profiles.

### Simulated Mole Fraction Profiles

Figure 2 presents simulation results for Systems 1 to 4 with unrestricted amount of C(s), as proposed by Halstead. Figure 3 presents simulation results for the same systems, but with zero amount of C(s), as proposed by Shirai and co-workers.

As seen in Figure 2, the simulation results when the amount of C(s) is unrestricted are the same for the four systems regardless of the assumptions about oil surrogates and presence of heavier gases. Also, a comparison of Figure 2 with the typical patterns of

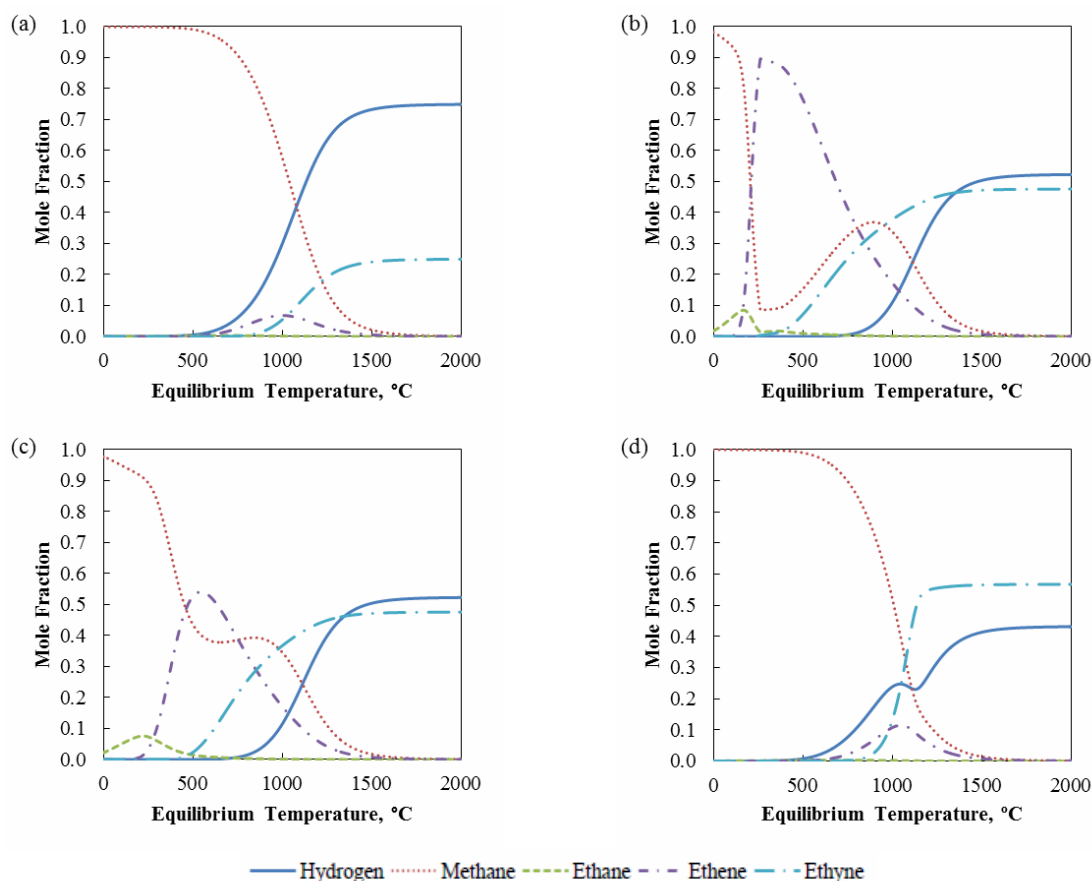
Table 1 reveals that the proposed systems are not able to represent the degradation of MIO when unrestricted equilibrium amount of C(s) is permitted, since only hydrogen and methane are non-trace species, which corroborates Shirai and co-workers' observations.



**Figure 2:** Simulation results for Systems 1 to 4 with unrestricted amount of C(s).

On the other hand, when comparing Figures 3a to 3d with the typical patterns, it is observed that the proposed systems may be able to qualitatively represent the degradation of MIO when no amount of C(s) exists in the equilibrium, due to the presence of the gases of interest as non-traces, even though the total absence of C(s) may not be considered a physically acceptable hypothesis.

Systems 2 and 3, with zero amount of C(s), seem to show the best performances since Figures 3b and 3c are the only plots to present a non-trace equilibrium amount of C<sub>2</sub>H<sub>6</sub>, as expected from Table 1. A more detailed evaluation of these two systems reveals that System 3 is possibly more adequate than System 2 in representing the degradation of MIO, since the latter (Figure 3b) presents an abrupt compositional change around the equilibrium temperature of 300 °C that is probably related to the lack of relevant species in the mid-range of molar mass.



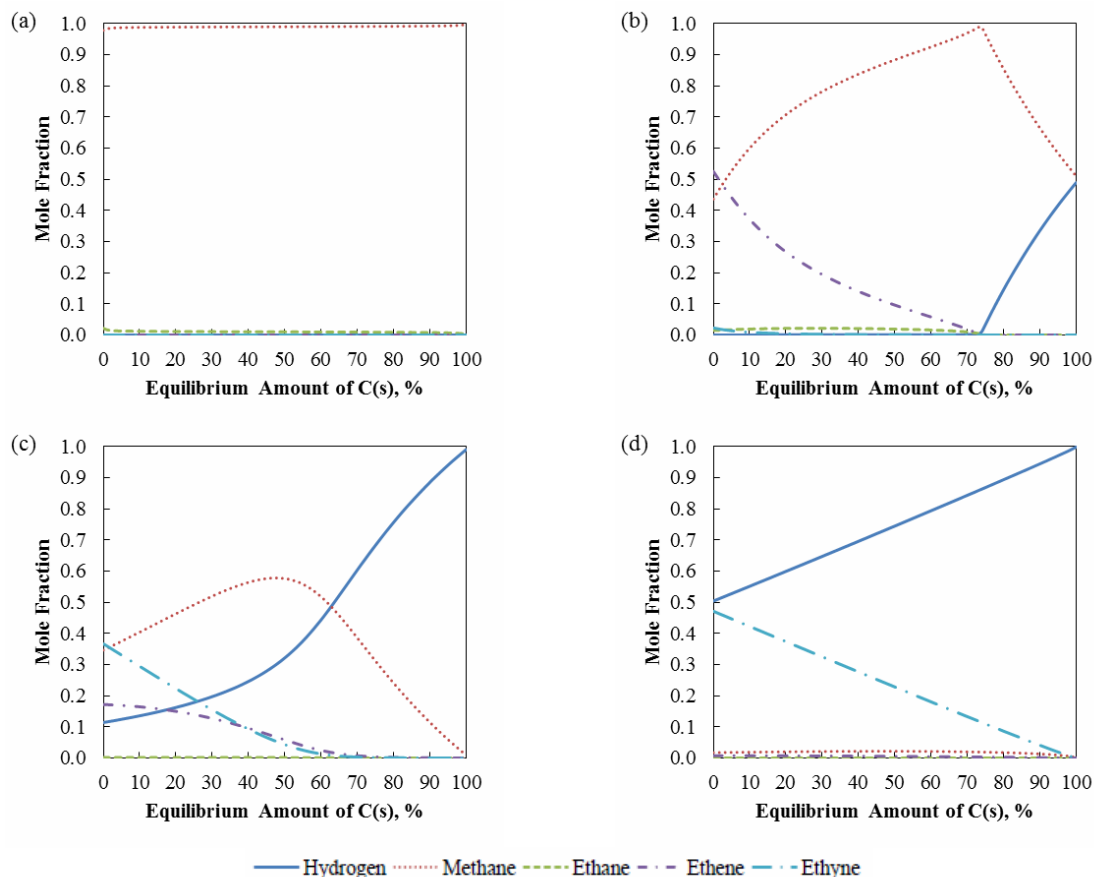
**Figure 3:** Simulation results for Systems 1 to 4 with zero amount of C(s). (a) System 1. (b) System 2. (c) System 3. (d) System 4.

Also, it is observed that despite being developed based on MIO compositional information, System 4 did not show the best performance in representing MIO thermal degradation. That is probably related to Shirai and co-workers' observations on the high stability of naphthenes and aromatics over the equilibrium temperature range of interest (Shirai *et al.*, 1977). Nonetheless, further studies on this subject might enlighten this discussion.

In the search for an alternative to the unlikely hypothesis of the total absence of C(s), simulations of intermediate scenarios of its equilibrium amount were carried out for System 3. Figure 4 presents the simulation results for System 3 when the equilibrium temperatures are kept constant and the restricted equilibrium amounts of C(s) vary from 0 to 100% of the unrestricted amounts, for equilibrium temperatures of 0 °C, 500 °C, 1000 °C and 1500 °C, respec-

tively. Simulation results obtained for equilibrium temperatures over 1500 °C showed very similar profiles to the 1500 °C profile and were suppressed.

Figures 4b to 4d show that, for a certain range of equilibrium temperatures, the mole fractions of some species in intermediate scenarios of the amount of C(s) differ from the base cases of 0% and 100% of the unrestricted amounts of C(s). Also, Figures 4b and 4c clearly indicate that the mole fraction of methane as a function of the restricted amount of C(s) is not a monotonic function. So, it is possible that the MIO thermal decomposition would be better represented in intermediate scenarios of the amount of C(s) for certain temperatures. In other words, the molar compositions obtained from these intermediate scenarios may be more adequate than those obtained from the zero amount of C(s) scenario, but with the advantage of providing the formation of some C(s), as expected.



**Figure 4:** Simulation results for System 3 with a constant equilibrium temperature. (a)  $T = 0$  °C. (b)  $T = 500$  °C. (c)  $T = 1000$  °C. (d)  $T = 1500$  °C.



### Analysis of the Proposed Model Performance

In order to quantify and evaluate the proposed model prediction quality, Table 3 presents the optimum mean relative errors of randomly selected cases for simulations with unrestricted amount of C(s), zero amount of C(s) and, as proposed, optimized amount of C(s). PD means partial discharges, D1 means discharges of low energy, D2 means discharges of high energy, T1/T2 means low/medium temperature thermal faults and T3 means high temperature thermal faults.

**Table 3: Mean relative errors of unrestricted, zero and optimized amount of C(s) scenarios for selected cases.**

Case	Mean relative errors, %		
	Unrestricted C(s) scenario	Zero C(s) scenario	Optimized C(s) scenario
PD.1	75.13	631.82	52.09
PD.2	77.26	437.56	45.79
PD.3	77.51	90.88	44.96
D1.1	82.67	77.59	53.56
D1.2	78.73	77.05	40.13
D1.3	85.29	51.20	33.85
D2.1	132.57	66.07	66.07
D2.2	88.35	77.55	55.27
D2.3	112.39	58.61	58.61
T1/T2.1	80.90	56.85	55.48
T1/T2.2	78.97	95.33	58.21
T1/T2.3	75.34	3059.77	64.00
T3.1	139.51	121.21	121.21
T3.2	843.14	461.48	461.48
T3.3	100.86	68.07	68.07

As expected, Table 3 shows that the optimized C(s) scenario leads to mean relative errors that are lower or, at least, equal to the results of the other approaches. Even though the proposed carbon-optimized model introduces an additional parameter to address the problem, it must not be forgotten that it also presents qualitative and fundamental improvements when compared to the unrestricted and zero amount of C(s) approaches, *i.e.*, it presents equilibrium molar compositions comparable to the typical patterns and accounts for the expected presence of C(s).

The mean relative errors obtained with the proposed approach varied from 33.85% in D1.3 to 461.48% in T3.2. The high temperature thermal faults stood out as the incipient fault type with the poorest adherence to IEC data, presenting the highest associated mean relative errors. The PD.2 case provides a good example of improvement in the adherence of the simulation results to reported data: the

prediction of the two-dimensional model resulted in a mean relative error of 45.79% while the unrestricted and zero amounts of C(s) simulations resulted in errors of 77.26% and 437.56%, respectively.

Extending the simulations to all 117 cases presented in IEC data, the restriction to the equilibrium amount of C(s) resulted in lower errors when compared to the errors of the scenarios with unrestricted and zero amounts of C(s) in 71.8% of the cases. In the other 28.2% of the cases, the minimum errors were obtained in zero amount of C(s) scenarios. In none of the 117 cases, the minimum error was obtained in an unrestricted amount of C(s) scenario. As stated before, the unrestricted amount of C(s) scenario leads to a thermodynamic equilibrium that, in fact, is not fully achieved and, generally, does not fit the reported data.

In all cases, the generalized high errors obtained are mainly due to the contribution of the excessively high relative deviations in the cases of extremely low reported mole fractions. All the same, as described before, relatively high errors were a possibility since IEC data present information from in-service equipment and not from specially designed experiments.

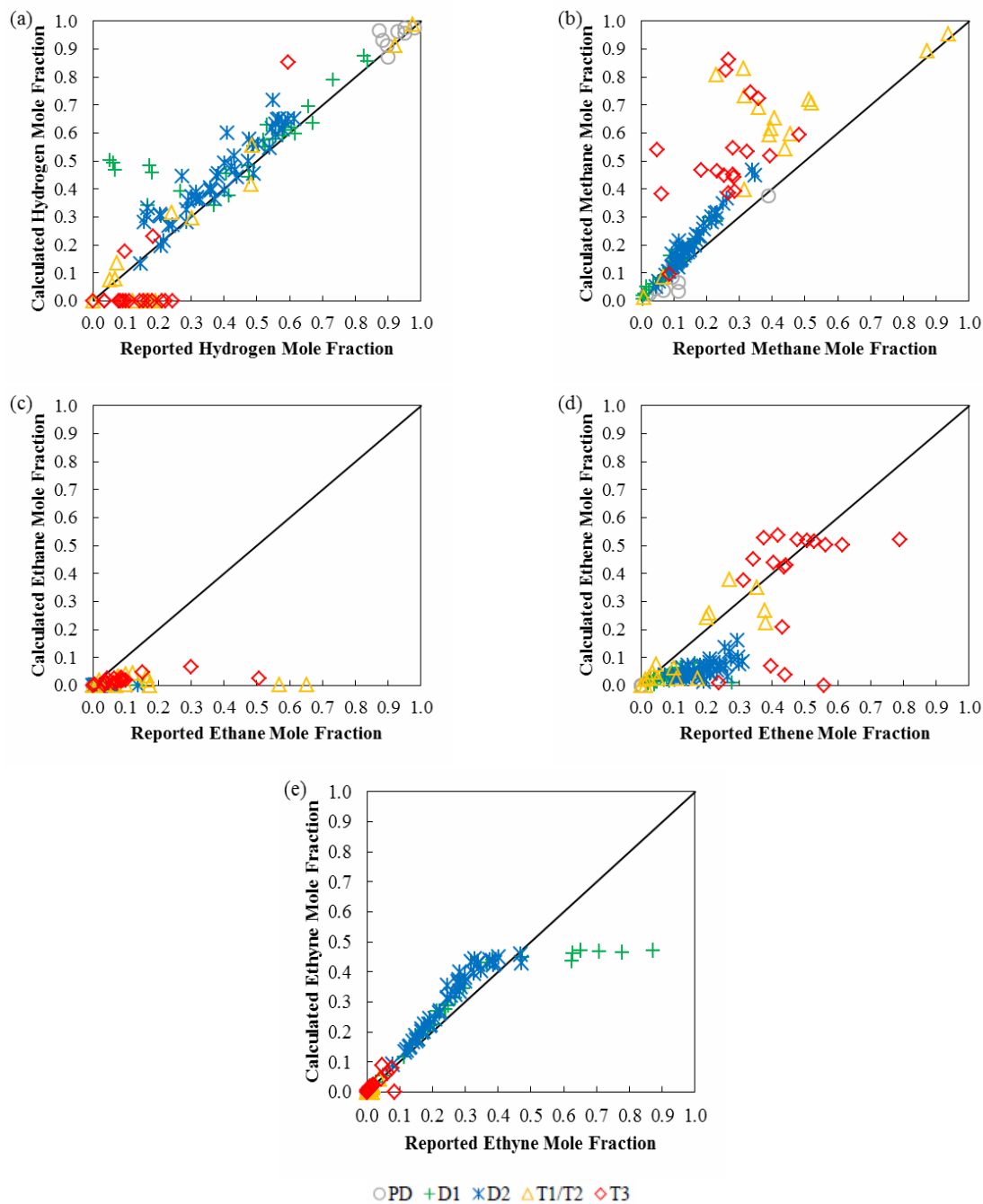
### Comparison of Calculated and Reported Mole Fractions

As described before, the solution of two-dimensional optimization problems led to the equilibrium temperature and the percentage of the equilibrium amount of C(s) that minimized the residue between the model prediction and the reported mole composition for each case in IEC data. Figure 5 presents plots of the optimum predicted mole fractions versus the reported mole fractions of the species of interest, allowing the evaluation of the two-dimensional model adequacy to IEC data. The different symbols identify the associated incipient faults types.

Figure 5a indicates that predicted hydrogen mole fractions show good agreement with reported data, except for high temperature thermal faults, where the model predicts an unreported absence of hydrogen. Figure 5b indicates that predicted methane mole fractions also show good agreement with the reported data, but, in many cases, the predicted values are greater than the reported data for thermal faults. Figure 5c indicates that predicted ethane mole fractions show poor agreement with the reported data for all incipient fault types: all model predicted values are much lower than the reported data. Figure 5d indicates that predicted ethene mole fractions show, overall, some agreement with the reported data, although the model seems to overestimate the mole

fractions for thermal faults and underestimate the mole fractions for electrical faults. Figure 5e indicates that predicted ethyne mole fractions show good agreement with reported mole fractions below 0.45: for all reported data above this value, the model pre-

dicts mole fractions around 0.45. It is also worthy to note that, except for the predictions of ethyne mole fractions, all predictions in high temperature thermal fault cases showed very poor agreement with the reported data.



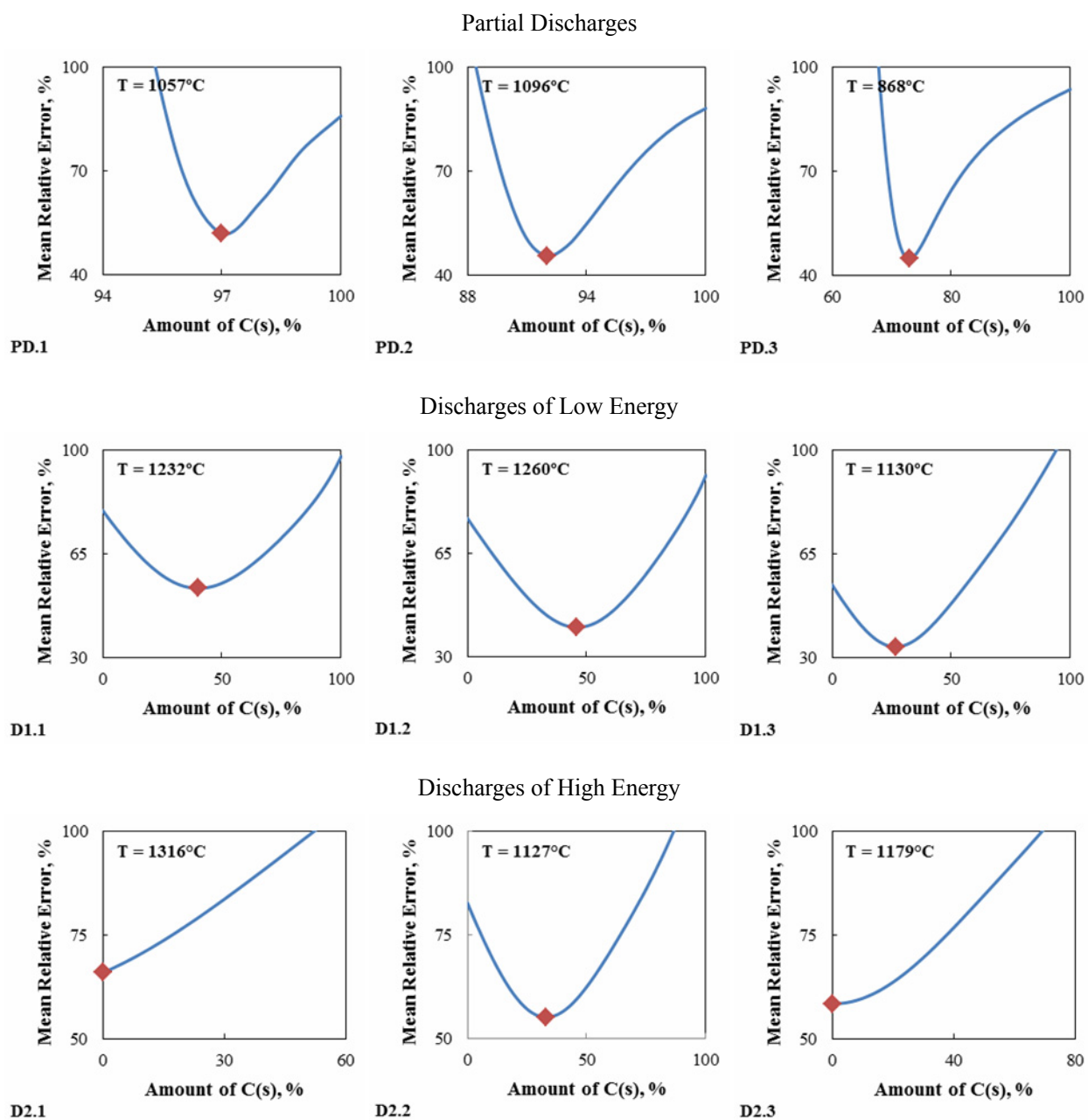
**Figure 5:** Model predicted versus reported mole fractions. (a) Hydrogen. (b) Methane. (c) Ethane. (d) Ethene. (e) Ethyne.

## Objective Function Profiles

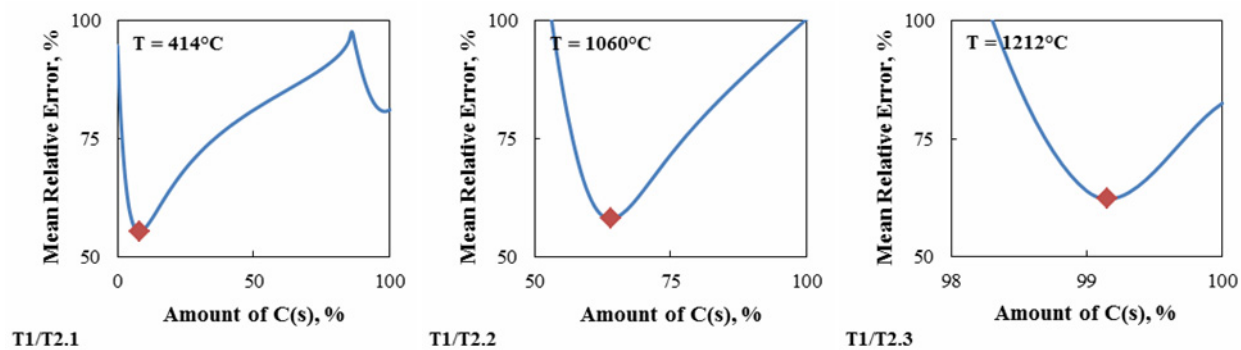
In order to expose the characteristics of the optimization problem and to evaluate the performance of the applied numerical method, Figure 6 presents the mean relative errors of the same cases in Table 3 as functions of the percentages of the equilibrium amounts of C(s). The

temperatures were kept constant at their optimum values.

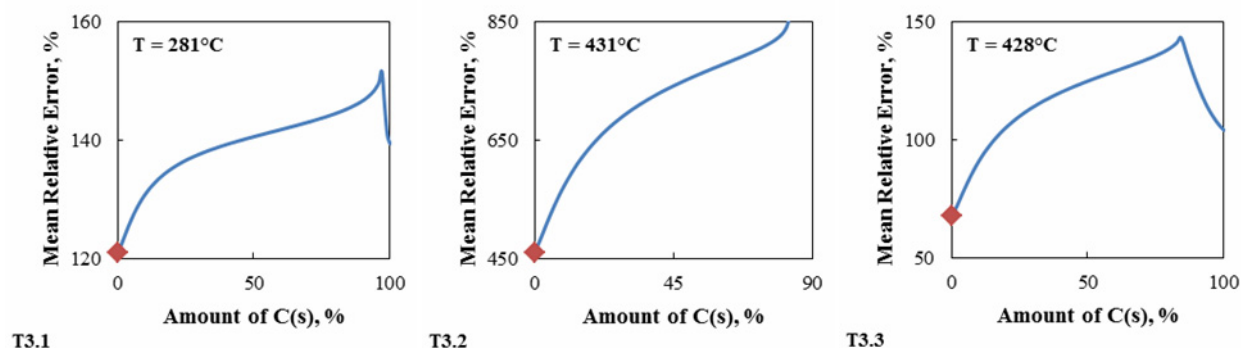
It is observed that the objective function showed different profiles, depending on the case, including the occurrence of local minimums. Also, it is interesting to observe once more that the minimum error could not be obtained for the unrestricted C(s) scenario in any of the cases.



## Low/medium Temperature Thermal Faults



## High Temperature Thermal Faults



**Figure 6:** Mean relative prediction errors as functions of the allowed equilibrium amounts of C(s) percentages with fixed temperatures.

## CONCLUSIONS

This paper presents a proposal of thermodynamic and compositional models for chemical equilibrium simulations of the thermal degradation of mineral insulating oil. The proposed carbon-optimized model was able to adapt to both hypotheses available in the literature for the equilibrium amount of C(s), *i.e.*, zero amount of C(s) and unrestricted amount of C(s). Also, the proposed model permitted simulations of intermediate scenarios regarding the equilibrium amount of C(s), which is intended to account for the kinetics of the phenomenon.

One-dimensional simulation results showing better adequacy to empirical data were obtained when mineral insulating oil was represented by  $C_{20}H_{42}$ , which degraded into 59 species and with zero equilibrium amount of C(s). The two-dimensional model, *i.e.*, when the equilibrium amount of C(s) could also be specified, made it possible to simulate intermediate scenarios of the amount of C(s) between the zero and the unrestricted amounts cases, thus avoiding the implausible hypothesis of the total absence of C(s) in

the equilibrium. The two-dimensional simulation results were also more adherent to empirical data than those obtained from classical models available in the literature.

The proposed carbon-optimized thermodynamic model proved to be an improvement in representing the reported data when an adequate compositional model was applied. It may be even possible to use the proposed model to develop a phenomenologically-based diagnostic method. Nevertheless, further investigations may be required to develop a more adequate degradation model, especially regarding the poor agreement of the predicted ethane mole fractions to the reported data and the high errors obtained in the predictions of high temperature thermal fault cases.

## ACKNOWLEDGMENT

Vinicius G. M. Cruz thanks Furnas Centrais Elétricas for encouraging the development of this work.

## NOMENCLATURE

$a$	number of atoms of an element in one molecule of a substance (dimensionless)
$C_P$	molar heat capacity at constant pressure ( $\text{J}\cdot\text{mol}^{-1}\cdot\text{K}^{-1}$ )
$G$	molar Gibbs energy ( $\text{J}\cdot\text{mol}^{-1}$ )
$H$	molar enthalpy ( $\text{J}\cdot\text{mol}^{-1}$ )
$n$	amount of substance (mol)
$P$	product of decomposition of a representative compound (dimensionless)
$R$	universal gas constant ( $\text{J}\cdot\text{mol}^{-1}\cdot\text{K}^{-1}$ )
$RC$	representative compound (dimensionless)
$T$	equilibrium temperature (K)

### Superscripts

$^\circ$	standard state
$0$	initial amount

### Subscripts

$C$	carbon
$f$	formation
$h$	heavy species
$H$	hydrogen
$i$	species index (all species except C(s))
$j$	species index (all species)
$k$	representative compound index
$l$	light species
$R$	restricted
$t$	total (all species except C(s))

### Greek Letters

$\lambda$	Lagrange multiplier (dimensionless)
-----------	-------------------------------------

## REFERENCES

- ASTM International, Electrical Insulating Liquids. Chelsea, Michigan (1994).
- ASTM International, Research Report RR # D27-1016: Inter-Laboratory Study to Establish Precision Statements for ASTM D3612, Standard Test Method for Analysis of Gases Dissolved in Electrical Insulating Oil by Gas Chromatography. West Conshohocken, Pennsylvania (2003).
- ASTM International, D923 – 07: Standard Practices for Sampling Electrical Insulating Liquids. West Conshohocken, Pennsylvania (2007).
- ASTM International, D3612 – 02 (2009): Standard Test Method for Analysis of Gases Dissolved in Electrical Insulating Oil by Gas Chromatography. West Conshohocken, Pennsylvania (2009).
- Barrett, K. A., Dissolved gas-in-oil analysis – an expert system. Proceedings of the 1989 International Conference of Doble Clients. Boston, Massachusetts (1989).
- Duval, M. and dePablo, A., Interpretation of gas-in-oil analysis using new IEC publication 60599 and IEC TC 10 databases. IEEE Electr. Insul. Mag., 17, 31-41 (2001).
- Fei, S. W. and Zhang, Z. B., Fault diagnosis of power transformer based on support vector machine with genetic algorithm. Expert Syst. Appl., 36, 11352-11357 (2009).
- Fei, S.-W., Wang, M.-J., Miao, Y.-B., Tu, J. and Liu, C.-L., Particle swarm optimization-based support vector machine for forecasting dissolved gases content in power transformer oil. Energy Convers. Manage., 50, 1604-1609 (2009).
- Halstead, W. D., Thermodynamic assessment of the formation of gaseous hydrocarbons in faulty transformers. J. Inst. Pet., 59, 239-241 (1973).
- Huang, Y. C. A., New data mining approach to dissolved gas analysis of oil-insulated power apparatus. IEEE Trans. Power Delivery, 18, 1257-1261 (2003).
- Institute of Electrical and Electronics Engineers, IEEE Std C57.104-2008: IEEE Guide for the Interpretation of Gases Generated in Oil-Immersed Transformers. New York (2009).
- International Electrotechnical Commission, IEC 60599:1999+A1:2007: Mineral Oil-Impregnated Electrical Equipment in Service – Guide to the Interpretation of Dissolved and Free Gases Analysis. Geneva, Switzerland (2007).
- Lowe, R. I., Artificial intelligence techniques applied to transformer oil dissolved gas analysis. Proceedings of the 1985 International Conference of Doble Clients. Boston, Massachusetts (1985).
- Miranda, V., Castro, A. R. G. and Lima, S., Diagnosing faults in power transformers with autoassociative neural networks and mean shift. IEEE Trans. Power Delivery, 27, 1350-1357 (2012).
- Poling, B. E., Prausnitz, J. M. and O'Connell, J. P., The Properties of Gases and Liquids. McGraw-Hill, New York (2001).
- Press, W. H., Teukolsky, S. A., Vetterling, W. T. and Flannery, B. P., Numerical Recipes: The Art of Scientific Computing. Cambridge University Press, Cambridge (2007).
- Rogers, R. R., IEEE and IEC codes to interpret incipient faults in transformers, using gas in oil analysis. IEEE Trans. Electr. Insul., EI-13, 349 (1978).

- Shirai, M., Shimoji, S. and Ishii, T., Thermodynamic study on the thermal decomposition of insulating oil. *IEEE Trans. Electr. Insul.*, EI-12, 272-280 (1977).
- Smith, J. M., Van Ness, H. C. and Abbott, M. M., *Introduction to Chemical Engineering Thermodynamics*. McGraw-Hill, New York (2004).
- Tomsovic, K., Tapper, M. and Ingvarsson, T. A., Fuzzy information approach to integrating different transformer diagnostic methods. *IEEE Trans. Power Delivery*, 8, 1638-1646 (1993).
- Wang, Z. and Liu, Y. A., Combined ANN and expert system tool for transformer fault diagnosis. *IEEE Trans. Power Delivery*, 13, 1224-1229 (1998).
- Wu, H., Li, X. and Wu, D., RMP neural network based dissolved gas analyzer for fault diagnostic of oil-filled electrical equipment. *IEEE Trans. Dielectr. Electr. Insul.*, 18, 495-498 (2011).
- Zhang, Y., Ding, X., Liu, Y. and Griffin, P. J., An artificial neural network approach to transformer fault diagnosis. *IEEE Trans. Power Delivery*, 11, 1836-1841 (1996).